*FEMS Microbiology Letters*, 2023, **370**, 1–8
DOI: 10.1093/femsle/fnad047
**Advance access publication date: 5 June 2023**
**Research Letter** – Environmental Microbiology and Microbial Ecology

# Cadmium effects on net $N_2O$ production by the deep-sea isolate *Shewanella loihica* PV-4

Leonor Pizarro[1,2], Catarina Magalhães[1,3], C. Marisa R. Almeida[1,4], Maria de Fátima Carvalho[1,5], Miguel Semedo[1,*,†]

[1]Interdisciplinary Centre of Marine and Environmental Research (CIIMAR), University of Porto, Matosinhos 4450-208, Portugal
[2]Faculty of Biotechnology, Catholic University of Portugal, Porto 4169-005, Portugal
[3]Department of Biology, Faculty of Sciences (FCUP), University of Porto, Porto 4169-007, Portugal
[4]Department of Chemistry and Biochemistry, Faculty of Sciences (FCUP), University of Porto, Porto 4169-007, Portugal
[5]Institute of Biomedical Sciences Abel Salazar (ICBAS), University of Porto, Porto 4050-313, Portugal
*Corresponding author. Interdisciplinary Centre of Marine and Environmental Research (CIIMAR), University of Porto, Matosinhos 4450-208, Portugal. E-mail: msemedo@ciimar.up.pt
†Present address: Interdisciplinary Centre of Marine and Environmental Research (CIIMAR), Terminal de Cruzeiros de Leixões, Av. General Norton de Matos s/n, 4450-208 Matosinhos, Portugal. Tel: +351 915587605.
**Editor:** [Serena Rinaldo]

## Abstract

Deep-sea mining may lead to the release of high concentrations of metals into the surrounding seabed, which can disturb important ecosystem functions provided by microbial communities. Among these, the production of $N_2O$ and its reduction to $N_2$ is of great relevance since $N_2O$ is an important greenhouse gas. Metal impacts on net $N_2O$ production by deep-sea bacteria are, however, currently unexplored. Here, we evaluated the effects of cadmium (Cd) on net $N_2O$ production by a deep-sea isolate, *Shewanella loihica* PV-4. We performed a series of Cd exposure incubations in oxic conditions and determined $N_2O$ fluxes during induced anoxic conditions, as well as the relative expression of the nitrite reductase gene (*nirK*), preceding $N_2O$ production, and $N_2O$ reductase gene (*nosZ*), responsible for $N_2O$ reduction. Net $N_2O$ production by *S. loihica* PV-4 exposed to Cd was strongly inhibited when compared to the control treatment (no metal). Both *nirK* and *nosZ* gene expression were inhibited in reactors with Cd, but *nirK* inhibition was stronger, supporting the lower net $N_2O$ production observed with Cd. The Cd inhibition of net $N_2O$ production observed in this study poses the question whether other deep-sea bacteria would undergo the same effects. Future studies should address this question as well as its applicability to complex communities and other physicochemical conditions, which remain to be evaluated.

**Keywords:** deep-sea, mining, metal contamination, denitrification, nitrous oxide, gene expression

## Introduction

Over the next few decades, deep-sea mining of earth minerals is expected to increase as demand is growing and the technical limitations of mining the deep ocean are being resolved. Over 29 exploration contracts already exist to mine locations in international waters, mostly aiming to extract minerals from manganese nodules, cobalt crusts, or massive sulfide deposits (Cuyvers et al. 2018, Miller et al. 2018). Deep-sea mining may pose environmental risks to benthic life that would otherwise be virtually undisturbed by human activities (Orcutt et al. 2020). The operation of heavy machinery on the ocean floor may lead to sediment restructure and mining metallic substrates may release toxic concentrations of metals, which can affect biological processes across various domains of life (Magalhães et al. 2011, Jordi et al. 2012, Semedo et al. 2012, Hauton et al. 2017). Cadmium (Cd) is one of the metals present in deep-sea ore deposits that may be released during deep-sea mining operations (Hauton et al. 2017). Due to its high toxic potential and to previously reported impacts in microbial metabolic and biogeochemical processes in different environments (Magalhães et al. 2007, Liu et al. 2016, Afzal et al. 2019, Broman et al. 2019), it is important to investigate Cd impacts on deep-sea microbial life.

Deep-sea microorganisms provide several ecosystem functions of great value to environmental sustainability (Orcutt et al. 2020). They are responsible for the majority of nutrient cycling in the deep-sea, methane production/oxidation, nitrous oxide production/reduction, and so forth. Nitrous oxide ($N_2O$) is a potent greenhouse gas predicted to have a major impact on the globe's climate over the next 100 years (Ravishankara et al. 2009, Neubauer and Megonigal 2015). The fine balance between its production and consumption in deep waters is of great relevance to the control of greenhouse gas emissions from the ocean, the largest ecosystem on earth (Miller et al. 2018, Bange et al. 2019). Denitrification, the stepwise reduction of nitrate ($NO_3^-$) and nitrite ($NO_2^-$) to nitric oxide (NO), nitrous oxide ($N_2O$), and dinitrogen gas ($N_2$), can be a source or sink of $N_2O$ due to its modularity (Graf et al. 2014). If the enzymes responsible for the steps preceding $N_2O$ formation, such as nitrite reductase (EC 1.7.1.4), are more abundant or active than the $N_2O$ reductase enzyme (EC 1.7.2.4.), responsible for $N_2O$ reduction, denitrification is a source. On the other hand, when $N_2O$ reductase is more abundant or active, denitrification becomes a sink. Nitrite reductase is encoded by *nirS* or *nirK* while $N_2O$ reductase is encoded by *nosZ*, with two distinct clades, *nosZI* and *nosZII* (Hallin et al. 2018). The relative expression of sources (*nirS* or *nirK*) vs. sinks (*nosZ*) will, ultimately, determine $N_2O$ fluxes in a particular environment or bacterial culture. While some studies report denitrification as an important pathway for $NO_3^-$ removal in deep-sea sediments (Xu et al. 2022) or deep-sea sponge grounds

**Received** 31 January 2023; **revised** 19 May 2023; **accepted** 1 June 2023

(Rooks et al. 2020), denitrification activity and gene expression regulation by deep-sea bacterial isolates is relatively understudied. In this work, we take a closer look at net $N_2O$ production (resulting from production and consumption) by a deep-sea isolate due to the current lack of evidence about its drivers in the deep-sea as well as their susceptibility to metal pollution.

It is reasonable to expect that denitrification and, consequently $N_2O$ production/reduction can be disturbed by the intensification of deep-sea mining. Increased metal exposure can lead to reduced microbial growth, denitrifying activity, and diversity of denitrifying microorganisms in various environments (Kandeler et al. 1996, Huang et al. 2008, Magalhães et al. 2011, Baptista et al. 2015). Even metals that are essential cofactors of microbial enzymes, such as copper in nitrous oxide reductase, can inhibit their reactions when environmental concentrations exceed a certain level (Magalhães et al. 2011, Glass and Orphan 2012). Indirect effects may also be relevant. For instance, metal availability and consequent oxidation in the deep seawater may decrease the pH, analogous to an acid mine drainage in terrestrial environments (Orcutt et al. 2020). Lower pH is known to inhibit $N_2O$ reduction by inhibition of *nosZ* gene expression or post-transcriptional interference (Liu, Frostegård and Bakken 2014; Samad et al. 2016, Gaimster et al. 2017), which may lead to increased $N_2O$ fluxes from deep-sea communities.

Despite the potential risk for increased mobilization and bioavailability of metals in deep-sea sediments related to mining activities, little is known about the impacts of metals on microbial life in the deep-sea. A few studies have addressed the toxic effects of metals in larger organisms in deep-sea conditions (low temperature and high pressure) and reported that the increased pressure and/or lower temperatures affected the toxicity potential of each metal (Hauton et al. 2017). For example, when a crustacean was exposed to copper and/or cadmium, the toxicity of copper increased at higher hydrostatic pressure but cadmium toxicity did not change with pressure (Brown et al. 2017). The colder temperatures and higher pressures of deep-sea conditions will likely affect the toxicity of metals to any living organism, however, the direction of that effect on microorganisms is currently unknown. In fact, to our knowledge, no studies with these metals have been performed so far with microorganisms isolated from the deep-sea and/or able to tolerate deep-sea conditions.

In this research, we attempted to initiate the investigation of metal impacts on denitrification and $N_2O$ metabolism in deep-sea microorganisms. The specific objective was to investigate the Cd impacts on net $N_2O$ production from *Shewanella loihica* PV-4, a deep-sea isolate carrying *nirK* and *nosZI* genes (Jones et al. 2013, Graf et al. 2014). To achieve this goal, we performed a series of exposure experiments with dissolved Cd and measured $N_2O$ concentration over time during induced anoxia. To further understand the potential impacts of the metal on the production and reduction of $N_2O$, we measured the relative expression of both *nirK* and *nosZ* genes in the same period.

## Material and methods

*Shewanella loihica* strain PV-4$^T$ (DSM 17748) was obtained from the German Collection of Microorganisms and Cell Cultures (DSMZ),

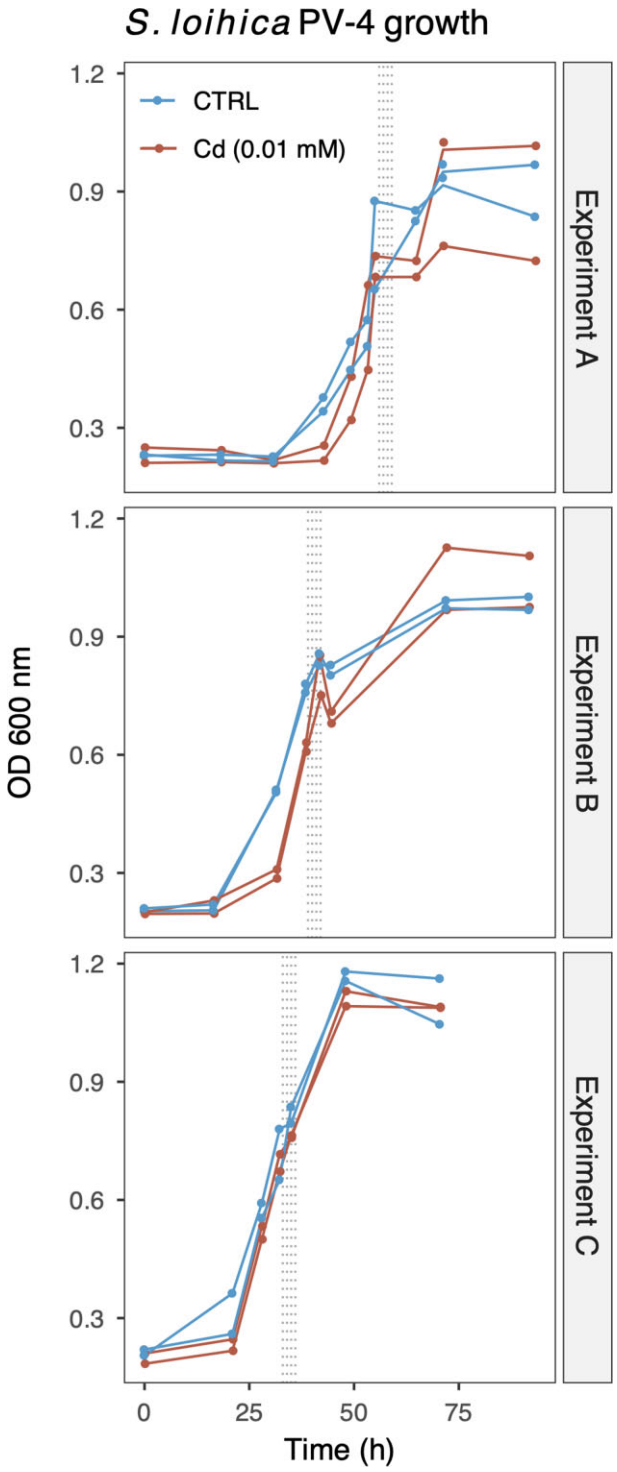


**Figure 1.** Optical density at 600 nm in the bioreactors during the exposure experiments with *S. loihica* PV-4 in oxic conditions. Each point represents the OD600 measurement from a single reactor at a given time point. The shaded area represents the 95% confidence interval of the locally estimated scatterplot smoothing (solid line). The dotted vertical lines represent the period when anoxia was induced for $N_2O$ and gene expression measurements.

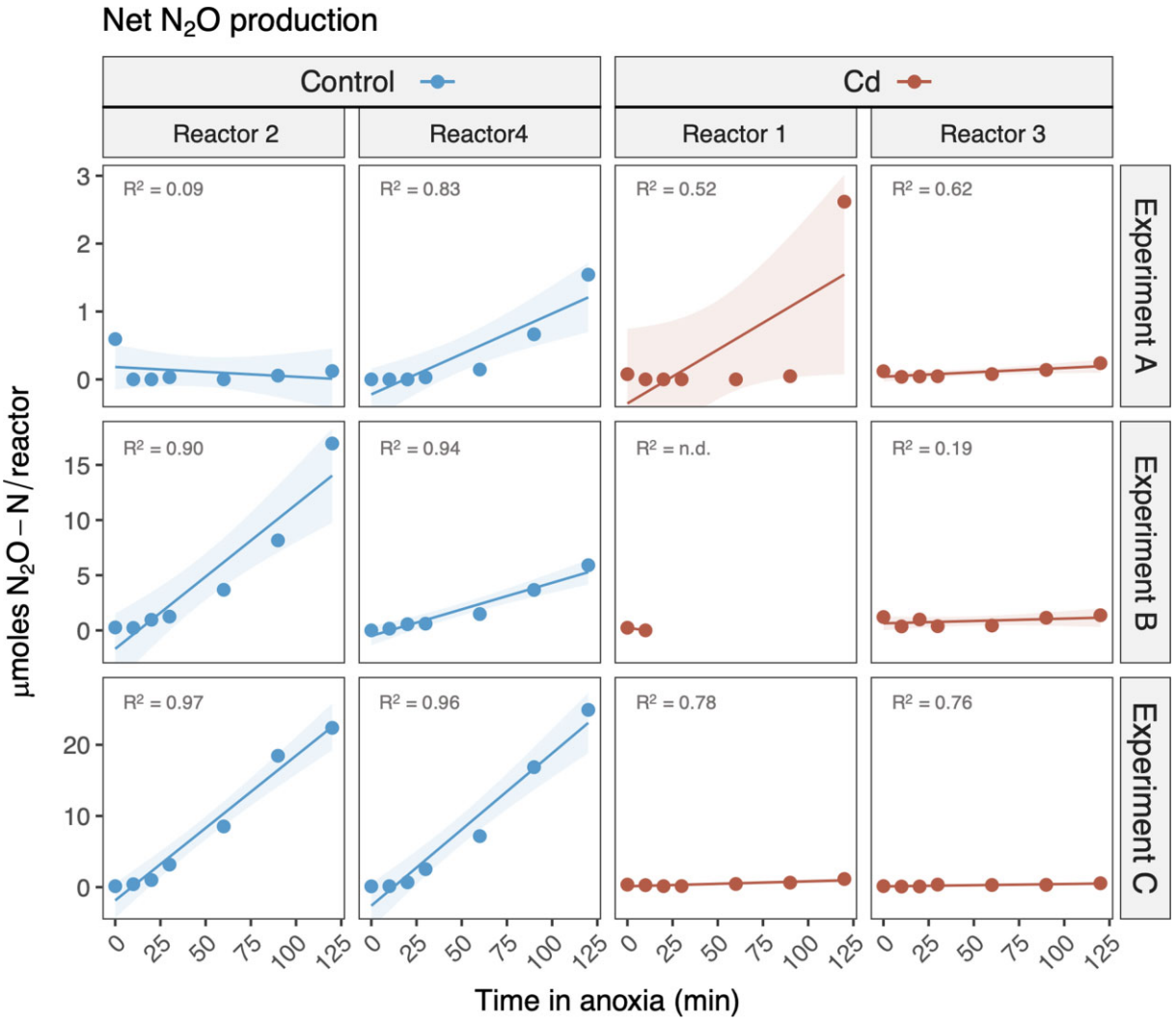


**Figure 2.** Nitrous oxide amount in the bioreactors during the exposure experiments with *S. loihica* PV-4. Each point represents the $N_2O$ measurement from a single reactor at a given time point during the anoxic period. The solid line represents the linear regression per reactor and the shaded area represents the 95% confidence interval. Calculated slopes and fluxes are presented in Table S4.

activated according to provided instructions, and stored at −80°C. From the frozen culture stock, *S. loihica* PV-4 was transferred to a Luria-Bertani (LB) agar plate and pre-grown at 28°C until obtaining enough inoculum biomass for the exposure experiments (around 9 days). All Cd exposure experiments were performed in bioreactors Bio-Xplorer 400P (HEL Group, London, United Kingdom). The system is composed of four independent bioreactors and continuously (every 20 seconds) monitors pH, temperature, pressure, dissolved oxygen (DO), and air mass flow for each individual bioreactor.

The pre-grown cultures were retrieved from the plates and transferred to around 15 mL of Marine Basal Media (MBM) to generate a dense inoculum to be added to the bioreactors. MBM is composed of a sea salts commercial mixture (20 g/L), 1 M Tris-HCl (71.25 mL/L) with pH adjusted to 7.5 with 6 N HCl, $K_2HPO_4.3H_2O$ (0.041 g/L), and $NH_4Cl$ (0.7125 g/L). Bioreactors were filled with 280 mL of MBM supplemented with 10 mM glucose as a carbon and electron source, 1 mM potassium nitrate ($KNO_3$) as electron acceptor when anoxic conditions were to be induced (see below), 0.01 mM cadmium chloride ($CdCl_2$), and 20% inoculum. Control treatments were done under the same conditions without adding $CdCl_2$. The Cd concentration used (0.01 mM, ca. 1.83 mg/L) is approximate to the effect range low (ERL) for this metal (Long et al. 1995) and did not inhibit *S. loihica* PV-4 growth in preliminary dose-response experiments (Fig. S1**,** Supplementary Material), which allow us to compare metabolic effects while dissociating effects on growth. Even though dissolved Cd concentrations in deep-sea water tend to be lower, within the nM range (Kádár et al. 2005, Janssen et al. 2014), ppm values have been previously detected in aragonite and calcite from deep-sea cold seeps (Feng and Chen 2015) or in hydrothermal sediments (Hu et al. 2017), which underscores the environmental relevance of the chosen concentrations in the deep-sea. Both control and cadmium treatments were replicated in two individual bioreactors per experiment and in three replicate experiments (experiments A, B, and C) since there are only four reactors available in the Bio-Xplorer 400P system. In total, six replicate incubations were performed for each treatment (3 experiments x 2 reactors).

Experiments A, B, and C started with synthetic compressed air flowing inside the bioreactors to allow *S. loihica* PV-4 aerobic growth. Cell growth was measured through optical density readings at 600 nm (OD600). When cultures reached the mid-exponential phase, gas supply was changed to $N_2$ (99.9999%) to create an anoxic environment and stimulate denitrifying condi-

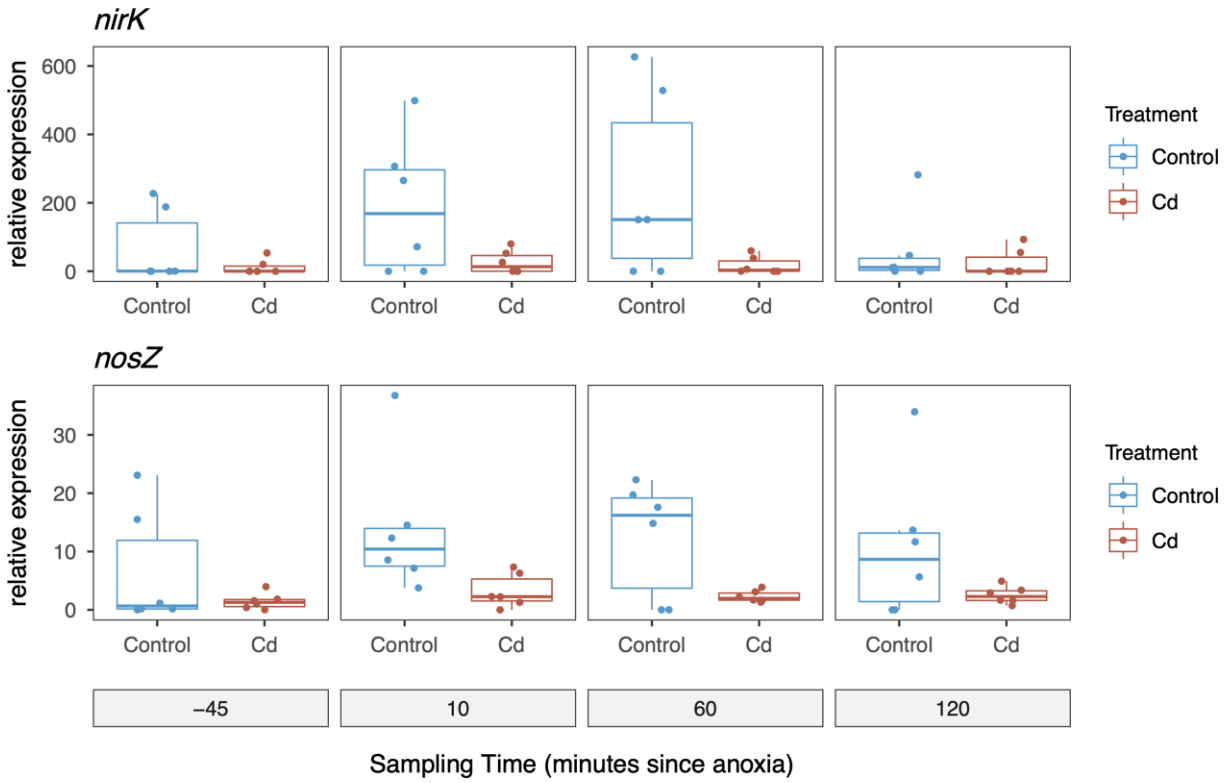


**Figure 3.** Relative expression of *nirK* and *nosZ* genes in *S. loihica* PV-4 grown with Cd at 0.01 mM (red) and without the metal (blue). Relative expression was estimated by normalizing gene transcript copy numbers by the average of *recA* and *rpoB* transcript copy numbers in each sample. The boxes represent the first and third quartiles, with median value bisecting each box. The whiskers extend to the largest/smallest value, excluding outliers (data beyond 1.5 x interquartile range).

tions. When the DO probe indicated an oxygen value close to zero, the reactors were sealed and started an interval headspace gas sampling at minutes 0, 10, 20, 30, 60, 90, and 120, for further quantification of headspace $N_2O$ and the respective fluxes. Liquid media samples (10 mL) for RNA extraction and gene expression measurements were taken during the same experiments (A, B, and C) immediately before turning the flowing gas to $N_2$ (around 45 mins. before reaching anoxia), and at minutes 10, 60, and 120 of anoxia. After the induced anoxic period and sample collection, the synthetic air supply was replenished and cells were allowed to grow until reaching the stationary phase.

At the beginning and at the end of experiments A and B, 4 mL of the growth media from control and Cd-treated reactors were taken to determine the dissolved Cd concentration. Each sample (collected into pre-decontaminated plastic vessels) was centrifuged to discard cell debris, and 40 μL of concentrated nitric acid was added. Cadmium was then directly measured by atomic absorption spectrophotometry with an air-acetylene flame (AAS-flame). To quantify Cd, a linear regression obtained with aqueous Cd standard solutions ranging from 0.025 to 3 mg/L was used. Blank solutions were always measured with no significant signal being detected.

For gaseous $N_2O$ quantification, 10 mL of headspace samples were taken using an outlet port in the bioreactors and stored in pre-evacuated 12 mL glass vials closed with rubber stoppers and aluminum rings. Nitrous oxide was measured and quantified within a few days by gas chromatography coupled with electron capture detection (GC-ECD). Similar glass vials were injected with 100 ppm $N_2O$ (gas mix X10A, 100 ppm $N_2O$ in 99.99% $N_2$) in the same day of collection and quantified to account for potential gas leaks. The GC-ECD was calibrated with a commercial $N_2O$ standard of 100 ppm and the coefficient of variation for 4–8 replicate injections was <0.085%, at different times during experiment run. Total amounts (μmol) of $N_2O$ in the reactors (gas and liquid phase) were calculated as previously described (Yoon et al. 2015; Kim, Park and Yoon 2017) using a dimensionless Henry's constant of 2.02 for $N_2O$ at 28°C (Sander 2015), corrected for the ionic strength of the media. Nitrous oxide fluxes were calculated for each reactor from the linear rate of concentration increase in the headspace during the 120-min sampling periods. For $R^2$ values of the linear regression lower than 0.80, we consider that there is no linear relationship, so the slope (and the flux) is considered null.

Relative expression of *nirK* and *nosZ* genes was measured in RNA extracted from the culture media. Despite the presence of the nitric oxide reductase gene (*nor*) in *S. loihica* PV-4 genome (Graf et al. 2014) we did not measure its expression in this work due to the high reactivity of NO and potentially transient nature of *norB* expression products. At each time-point (−45, 10, 60, and 120 mins after reaching anoxia), 10 mL liquid samples were taken and immediately centrifuged for cells harvesting (5000 *g*, 10 min, 4°C). The supernatant was discarded, and the cells pellet washed with 10 mL PBS 1X. The washed pellet was flash frozen in liquid nitrogen and stored at −80°C until RNA extraction. The tubes used during cell precipitation and washing were kept on ice, whenever possible to minimize RNA degradation.

RNA extraction was performed with RNeasy Plus Mini Kit (Qiagen), following manufacturer's protocol. Extracted RNA concentration and quality was assessed using a DeNovix DS-11 FX spectrophotometer, and genomic DNA was removed with the RapidOut DNA Removal Kit (Thermo Scientific). RNA purity (i.e.

without DNA) was confirmed through negative PCR amplification of the recombinase A gene (*recA*). Treated RNA (114 ng) was used for cDNA synthesis using QuantiNovaTM Reverse Transcription Kit (Qiagen). Resultant cDNA was stored at −20°C until further use. Transcript copy numbers of *nirK*, *nosZ*, and of two reference genes (*recA* and *rpoB*) were determined by real-time quantitative PCR (qPCR). The two reference genes used have been widely used and previously validated in different bacterial expression studies, including with *Shewanella* species (Rocha et al. 2015, Liu et al. 2018). In our study, the difference in the average Ct value between treatments (control vs. Cd) was 0.7 and 1.4 for *recA* and *rpoB*, respectively. Primers for *nirK* and *nosZ* genes were previously designed (Yoon et al. 2015) and primers for the reference genes *recA* and *rpoB* were designed in this study, using Primer-BLAST (Ye et al. 2012). A list of the chosen primer sets and the qPCR cycling conditions as well as the reaction components are displayed in Table S1 (Supplementary Material). Gene standards of *nirK*, *nosZ*, *recA*, and *rpoB* for qPCR were prepared by PCR of extracted DNA from a colony of *S. loihica* PV-4 growing in LB Agar. PCR products were purified using the NZYGelpure kit (NZYTech), according to manufacturer instructions, and quantified with a Qubit fluorometer (Thermo Scientific). For every qPCR plate, fresh standard dilutions were prepared, accounting for eight standards in total, ranging from $10^2$ to $10^9$ copies/μL. Relative expression of *nirK* and *nosZ* genes was calculated by dividing their estimated copy numbers per well by the average copy numbers of the reference genes *recA* and *rpoB*.

Normality of calculated $N_2O$ fluxes was evaluated with Q–Q plots. Since fluxes displayed large departures from normality, a non-parametric test (unpaired two-sample Mann–Whitney–Wilcoxon) was used to identify significant differences between control and Cd-treated samples. Differences in the relative expression of *nirK* and *nosZ* genes between control and Cd-treated samples were tested with two-way analysis of variance (ANOVA) with sampling time (−45, 10, 60, and 120 min) and treatment (Control, Cd) as fixed factors. Normality and homoscedasticity were assessed with Q–Q and residual plots. Relative expression of both genes was log-transformed to meet ANOVA assumptions. Significant relationships for all tests were considered at $\alpha < 0.05$. Statistical analyses and data visualization were conducted in the R environment (version 4.1.1 Copyright 2015 The R Foundation for Statistical Computing).

## Results and discussion

The physicochemical conditions observed during the experiments were similar in both Cd-treated and control reactors. Temperature was constant at 28°C while pH varied between 6.9 and 7.9 (Fig. S2, Supplementary Material). It is worth noticing that the largest pH change was observed after sealing the reactors for inducing anoxia. The interruption of gas exchange in the headspace may have led to $CO_2$ accumulation with the consequent pH decrease in the media. Dissolved Cd in the media was quantified to confirm metal exposure at the target concentration (Table S2, Supplementary Material). Cadmium (Cd) concentrations measured at the beginning of the experiment in metal-treated bioreactors ($1.67 \pm 0.06$ mg/L) was approximate to the target Cd concentration of 1.83 mg/L (0.01 mM). At the end of the experiment, however, Cd concentration dropped to an average of $0.69 \pm 0.05$ mg/L, less than half of the initial concentration. The sharp decline in dissolved Cd concentration could have been caused by multiple mechanisms that are frequently observed during bacterial incubations with dissolved metals, such as adsorption to bacterial cells (Mullen et al. 1989) or sulfide particle precipitation (Janssen et al. 2014, Ma and Sun 2021). Biological strategies that may lead to precipitation can also be activated by bacteria to increase metal resistance, such as biofilm formation (Ma and Sun 2021) or the production of external vesicles, that is known to be stimulated upon exposure to high metal concentrations (Lima et al. 2022). *Shewanella loihica* PV-4, for instance, was previously shown to be a strong oxidizer of another transition metal, Mn, in aerobic conditions, with the ability to form metal finely grained particles (Wright et al. 2016).

The growth curves of *S. loihica* PV-4 during the exposure experiments are shown in Fig. 1. The three replicate experiments followed a typical bacterial growth curve with three phases (lag, exponential, and stationary). The beginning of the exponential phase, however, was slightly different between experiments, with experiment C and B starting a few hours earlier than experiment A due to shorter lag phases, especially in experiment C. Besides the earlier beginning of the exponential phase, experiment C also displayed steeper slopes during the exponential phase, hence, higher maximum growth rates (Table S3, Supplementary Material). Due to these differences, the sampling period of each experiment (when anoxia was induced) was adjusted so that the growth phase and biomass (assessed by the OD readings) were similar between experiments. The OD values of each reactor when anoxia were induced was between 0.6 and 0.9 for all reactors in each experiment.

The Cd exposure effects on growth were similar in the three replicate experiments. Despite a slight delay in the start of the exponential phase in Cd-treated reactors, when compared to control, the metal did not inhibit growth of *S. loihica* PV-4 at the test concentration (0.01 mM). The calculated maximum growth rates were very similar between control and Cd-treated reactors across the three experiments (Table S3, Supplementary Material). This observation was expected, based on our preliminary dose-response experiment, which showed growth inhibition only at the Cd concentration of 0.05 mM or higher (Fig. S1, Supplementary Material). The absence of growth inhibition at 0.01 mM indicates that *S. loihica* PV-4 may be relatively resistant to Cd, since the same metal concentration in the media can be lethal to other model bacteria, such as *Escherichia coli* K-12 (Ferianc et al. 1998). Nevertheless, it is important to have in mind that *S. loihica* PV-4 relative resistance to Cd is limited. For instance, *S. loihica* PV-4 is far more sensitive than some bacteria isolated from Cd-polluted soils, that presented minimum inhibitory concentrations as high as 6 mM (Yu et al. 2021), and moderately more sensitive than some photosynthetic purple bacteria (Mohamed Fahmy Gad El-Rab et al. 2006) or even human pathogens, such as *Campylobacter jejuni* (Kaakoush et al. 2008). To our knowledge, no other deep-sea isolates have been tested against Cd exposure in growth media, even though it is reasonable to expect that deep-sea bacteria may be more resistant than shallower counterparts since Cd concentrations are known to increase with depth in the ocean water column (Xu and Morel 2013, Janssen et al. 2014). However, the overall susceptibility or resistance of deep-sea bacterial growth to metals is still poorly understood and its further investigation is out of the scope of this work, which focus on the Cd effects on $N_2O$ metabolism.

The $N_2O$ amounts in control and Cd-treated reactors during anoxia are shown in Fig. 2. Positive $N_2O$ fluxes were only detected in control reactors, while Cd-treated reactors consistently had $R^2$ values < 0.80 for the linear increase over time, hence, null fluxes (Table S4, Supplementary Material). A significant effect of treatment was observed in the calculated $N_2O$ fluxes (Mann–Whitney-Wilcoxon test, $P = 0.017$). Taking the three replicate experiments

into account, the average $N_2O$ fluxes were 0.101 ± 0.039 μmoles $N_2O$-N/min in control reactors and 0 μmoles $N_2O$-N/min in Cd-treated reactors, strongly suggesting that Cd might inhibit net $N_2O$ production in this deep-sea isolate. Besides the overall difference between control and Cd-treated reactors, we must also note that the $N_2O$ fluxes in control reactors were considerably variable between experiments, with much lower fluxes in experiment A (especially reactor 2), when compared to experiments B and C (Table S4, Supplementary Material). The lower fluxes observed in experiment A are probably due to the slightly later stage of growth when anoxia was induced (Fig. 1). The later stage of exponential growth could represent a lower amount of remaining glucose in the media (electron and C source), which would explain the lower $N_2O$ fluxes observed in experiment A.

As opposed to Fe or Cu, necessary for the catalytic activity of $NO_2^-$ and $N_2O$ reductase enzymes and potential direct impact on enzyme activity (Glass and Orphan 2012, Giannopoulos et al. 2020), Cd is not known to be a structural component of these metalloenzymes. Thus, Cd effects on $N_2O$ production and consumption are expected to be associated with cellular toxic effects, such as effects on cell growth, metabolism, and oxidative stress (Kaakoush et al. 2008, Behera et al. 2014, Cheng et al. 2022) as well as community effects, such as changes in microbial community structure and diversity in the environment (Yu et al. 2021, Sun et al. 2022). To our knowledge, no previous studies have investigated the effects of Cd on $N_2O$ metabolism using pure cultures or bacterial isolates. However, a few studies have investigated the same impacts on complex microbial communities. Using estuarine sediments, a previous study has found inhibited $N_2O$ reduction with consequent increase in net $N_2O$ production after Cd exposure (Magalhães et al. 2007), while others have found Cd stimulation of $N_2O$ reduction with an increase in $N_2$ production and no change in net $N_2O$ production in marine sediments (Broman et al. 2019). In metal polluted soils, researchers have found inhibited net $N_2O$ production, when compared to background soil, although these effects may change over time (Liu et al. 2016, Afzal et al. 2019). The contrasting results may be due to multiple factors, such as different environmental contexts, organic content, dose of exposure, etc. For instance, the Cd effects on total denitrification from wetland sediments was shown to be dose-dependent, with inhibitory effects being observed only at concentrations higher than 500 mg/Kg of sediment, with no effect at 100 mg/Kg (Sakadevan et al. 1999). Regarding deep-sea microbial communities, no studies have addressed this question so far, although this is a relevant investigation considering the emergence of deep-sea mining activities and potential release of trace metals.

To help unveiling the cellular mechanisms driving the inhibitory effect of Cd on net $N_2O$ production, we quantified the relative expression of the *nirK* and *nosZ* genes by qPCR (Fig. 3). The relative expression of both genes was lower in Cd-treated reactors than in control (mean and SEM values per treatment: $nirK_{CTRL}$ = 140 ± 39, $nirK_{Cd}$ = 20.2 ± 6.0; $nosZ_{CTRL}$ = 10.9 ± 2.2, $nosZ_{Cd}$ = 2.38 ± 0.38), with a significant effect of treatment detected in both genes (2-way ANOVA, *P*-value (*nirK*) = 0.0444; *P*-value (*nosZ*) = 0.00393). The inhibition of *nirK* relative expression, however, was stronger than the inhibition observed for the *nosZ* gene, resulting in a lower *nirK/nosZ* ratio in Cd-treated reactors, when compared to control ($nirK/nosZ_{CTRL}$ = 12.8, $nirK/nosZ_{Cd}$ = 8.49). These results contribute to explain the inhibitory effect of Cd on net $N_2O$ production, since a lower *nirK/nosZ* ratio supports a lower production to reduction potential. Recent studies have also reported that Cd decreases the number of *nirK* and *nosZ* transcripts in soil and marine sediment communities (Afzal et al. 2019, Broman et al. 2019) as well as decreased abundances of *nirK* and *nosZ* genes in soils contaminated with a mixture of trace metals, including Cd (Liu et al. 2016). Our study provides additional evidence that Cd exposure may inhibit *nirK* and *nosZ* gene expression at the individual strain level. Additionally, our results strongly suggest that this inhibition may be particularly stronger for *nirK* than for *nosZ*, with consequences for net $N_2O$ production. Interestingly, other researchers have found a stronger inhibitory effect of soil metal pollution on *nirK* gene abundance than *nosZ* (Liu et al. 2016), which suggests that our results may be transposable to complex communities.

In conclusion, we show here that Cd inhibits net $N_2O$ production in *S. loihica* PV-4 at levels near the ERL. Furthermore, we found that this inhibition is associated with the decrease in *nirK/nosZ* relative expression, suggesting that *nirK* gene expression may be more susceptible than *nosZ* to Cd exposure. It is important, however, to have in mind that our study was limited to a single bacterial strain. Since these effects have not been investigated in other pure cultures, future research should investigate whether our findings are specific to a few strains or observed across a wide range of taxa. Due to the emergence of deep-sea mining, investigating other deep-sea isolates could be of great environmental relevance. Additionally, the observed impacts of Cd exposure should also be investigated with deep-sea environmental communities as well as in deep-sea physicochemical conditions, such as high hydrostatic pressure and low temperature.

## Supplementary data

Supplementary data are available at *FEMSLE* online.

***Conflict of interest statement.*** None declared.

## Funding

This project has received funding from the European Union's Horizon 2020 research and innovation programme under the Marie Sklodowska-Curie grant agreement No 101038095. This work was also supported by the project ATLANTIDA (NORTE-01-0145-FEDER-000040), supported by the North Portugal Regional Operational Program (NORTE2020), under the PORTUGAL 2020 Partnership Agreement and through the European Regional Development Fund (ERDF).

## References

Afzal M, Yu M, Tang C *et al.* The negative impact of cadmium on nitrogen transformation processes in a paddy soil is greater under non-flooding than flooding conditions. *Environ Int* 2019;**129**:451–60.

Bange HW, Arévalo-Martínez DL, de la PM *et al.* A harmonized nitrous oxide (N 2 O) ocean observation network for the 21st century. *Front Mar Sci* 2019;**6**:1–10. doi: 10.3389/fmars.2019.00157.

Baptista MS, Miller RJ, Halewood ER *et al.* Impacts of silver nanoparticles on a natural Estuarine Plankton community. *Environ Sci Technol* 2015;**49**:12968–74.

Behera M, Dandapat J, Rath CC. Effect of heavy metals on growth response and antioxidant defense protection in *Bacillus cereus*. *J Basic Microbiol* 2014;**54**:1201–9.

Broman E, Motwani NH, Bonaglia S *et al.* Denitrification responses to increasing cadmium exposure in Baltic Sea sediments. *Aquat Toxicol* 2019;**217**:105328.

Brown A, Thatje S, Hauton C. The effects of temperature and hydrostatic pressure on metal toxicity: insights into toxicity in the deep sea. *Environ Sci Technol* 2017;**51**:10222–31.

Cheng G, Ding H, Chen G *et al.* Effects of cadmium sulfide nanoparticles on sulfate bioreduction and oxidative stress in desulfovibrio desulfuricans. *Bioresour Bioprocess* 2022;**9**:35.

Cuyvers L, Berry W, Kristina G *et al. Deep Seabed Mining: A Rising Environmental Challenge*. Gland, Switzerland: IUCN and Gallifrey Foundation, 2018.

Feng D, Chen D. Authigenic carbonates from an active cold seep of the northern South China Sea: new insights into fluid sources and past seepage activity. *Deep Sea Res Part II* 2015;**122**:74–83.

Ferianc P, Farewell A, Nyström T. The cadmium-stress stimulon of *Escherichia coli* K-12. *Microbiology (N Y)* 1998;**144**:1045–50.

Gaimster H, Alston M, Richardson DJ *et al.* Transcriptional and environmental control of bacterial denitrification and N2O emissions. *FEMS Microbiol Lett* 2017;**365**:1–8. doi: 10.1093/femsle/fnx277.

Giannopoulos G, Hartop KR, Brown BL *et al.* Trace metal availability affects greenhouse gas emissions and microbial functional group abundance in freshwater wetland sediments. *Front Microbiol* 2020;**11**:1–12.

Glass J, Orphan V. Trace metal requirements for microbial enzymes involved in the production and consumption of methane and nitrous oxide. *Front Microbio* 2012;**3**.

Graf DRH, Jones CM, Hallin S. Intergenomic comparisons highlight modularity of the denitrification pathway and underpin the importance of community structure for N2O emissions. *PLoS One* 2014:1–20.

Hallin S, Philippot L, Löffler FE *et al.* Genomics and ecology of novel N2O-reducing microorganisms. *Trends Microbiol* 2018;**26**:43–55.

Hauton C, Brown A, Thatje S *et al.* Identifying toxic impacts of metals potentially released during deep-sea mining-A synthesis of the challenges to quantifying risk. *Front Mar Sci* 2017;**4**:1–13. doi: 10.3389/fmars.2017.00368.

Hu Q, Zhang X, Jiang F *et al.* Geochemical characteristics of hydrothermal sediments from Iheya North Knoll in the Okinawa Trough. *Chin J Ocean Limnol* 2017;**35**:947–55.

Huang A, Chen H, Chen L *et al.* Effects of Cd(II) and Cu(II) on microbial characteristics in 2-chlorophenol-degradation anaerobic bioreactors. *Journal of Environmental Sciences* 2008;**20**:745–52.

Janssen DJ, Conway TM, John SG *et al.* Undocumented water column sink for cadmium in open ocean oxygen-deficient zones. *Proc Natl Acad Sci USA* 2014;**111**:6888–93.

Jones CM, Graf DRH, Bru D *et al.* The unaccounted yet abundant nitrous oxide-reducing microbial community: a potential nitrous oxide sink. *ISME J* 2013;**7**:417–26.

Jordi A, Basterretxea G, Tovar-Sánchez A *et al.* Copper aerosols inhibit phytoplankton growth in the Mediterranean Sea. *Proc Natl Acad Sci USA* 2012;**109**:21246–9.

Kaakoush NO, Raftery M, Mendz GL. Molecular responses of *Campylobacter jejuni* to cadmium stress. *FEBS J* 2008;**275**:5021–33.

Kádár E, Costa V, Martins I *et al.* Enrichment in trace metals (Al, Mn, Co, Cu, Mo, Cd, Fe, Zn, Pb and Hg) of macro-invertebrate habitats at hydrothermal vents along the Mid-Atlantic ridge. *Hydrobiologia* 2005;**548**:191–205.

Kandeler E, Kampichler C, Horak O. Influence of heavy metals on the functional diversity of soil microbial communities. *Biol Fertil Soils* 1996;**23**:299–306.

Kim H, Park D, Yoon S. pH control enables simultaneous enhancement of nitrogen retention and N2O reduction in Shewanella loihica strain PV-4. *Front Microbiol* 2017;**8**: DOI: 10.3389/fmicb.2017.01820.

Lima S, Matinha-Cardoso J, Giner-Lamia J *et al.* Extracellular vesicles as an alternative copper-secretion mechanism in bacteria. *J Hazard Mater* 2022;**431**:128594.

Liu B, Frostegård Å, Bakken LR. Impaired Reduction of N2O to N2 in Acid Soils Is Due to a Posttranscriptional Interference with the Expression of nosZ. *mBio* 2014;**5**:e01383–14.

Liu S, Meng C, Xu G *et al.* Validation of reference genes for reverse transcription real-time quantitative PCR analysis in the deep-sea bacterium Shewanella psychrophila WP2. *FEMS Microbiol Lett* 2018;**365**:fny048.

Liu Y, Liu Y, Zhou H *et al.* Abundance, composition and activity of denitrifier communities in metal polluted paddy soils. *Sci Rep* 2016;**6**:19086.

Long ER, Macdonald DD, Smith SL *et al.* Incidence of adverse biological effects within ranges of chemical concentrations in marine and estuarine sediments. *Environ Manage* 1995;**19**:81–97.

Ma N, Sun C. Cadmium sulfide nanoparticle biomineralization and biofilm formation mediate cadmium resistance of the deep-sea bacterium *pseudoalteromonas* sp.MT33b. *Environ Microbiol Rep* 2021;**13**:325–36.

Magalhães C, Costa J, Teixeira C *et al.* Impact of trace metals on denitrification in estuarine sediments of the Douro River estuary, Portugal. *Mar Chem* 2007;**107**:332–41.

Magalhães CM, Machado A, Matos P *et al.* Impact of copper on the diversity, abundance and transcription of nitrite and nitrous oxide reductase genes in an urban European estuary. *FEMS Microbiol Ecol* 2011;**77**:274–84.

Miller KA, Thompson KF, Johnston P *et al.* An overview of seabed mining including the current state of development, environmental impacts, and knowledge gaps. *Front Mar Sci* 2018;**4**:1–24. doi: 10.3389/fmars.2017.00418.

Mohamed Fahmy Gad El-Rab S, Abdel-Fattah Shoreit A, Fukumori Y. Effects of Cadmium stress on growth, morphology, and protein expression in *Rhodobacter capsulatus* B10. *Biosci Biotechnol Biochem* 2006;**70**:2394–402.

Mullen MD, Wolf DC, Ferris FG *et al.* Bacterial sorption of heavy metals. *Appl Environ Microbiol* 1989;**55**:3143–9.

Neubauer SC, Megonigal JP. Moving beyond global warming potentials to quantify the climatic role of ecosystems. *Ecosystems* 2015;**18**:1000–13.

Orcutt BN, Bradley JA, Brazelton WJ *et al.* Impacts of deep-sea mining on microbial ecosystem services. *Limnol Oceanogr* 2020;**65**:1489–1510. doi: 10.1002/lno.11403.

Ravishankara AR, Daniel JS, Portmann RW. Nitrous oxide (N2O): the dominant ozone-depleting substance emitted in the 21st century. *Science (1979)* 2009;**326**:123–5.

Rocha DJP, Santos CS, Pacheco LGC. Bacterial reference genes for gene expression studies by RT-qPCR: survey and analysis. *Antonie Van Leeuwenhoek* 2015;**108**:685–93.

Rooks C, Fang JK-H, Mørkved PT *et al.* Deep-sea sponge grounds as nutrient sinks: denitrification is common in boreo-arctic sponges. *Biogeosciences* 2020;**17**:1231–45.

Sakadevan K, Zheng H, Bavor HJ. Impact of heavy metals on denitrification in surface wetland sediments receiving wastewater. *Water Sci Technol* 1999;**40**:349–55.

Samad MDS, Biswas A, Bakken LR *et al.* Phylogenetic and functional potential links pH and N2O emissions in pasture soils. *Sci Rep* 2016;**6**:35990.

Sander R. Compilation of Henry's law constants (version 4.0) for water as solvent. *Atmos Chem Phys* 2015;**15**:4399–981.

Semedo M, Reis-Henriques MA, Rey-Salgueiro L *et al.* Metal accumulation and oxidative stress biomarkers in octopus (*Octopus vulgaris*) from Northwest Atlantic. *Sci Total Environ* 2012;**433**:230–7.

Sun H, Shao C, Jin Q *et al.* Effects of cadmium contamination on bacterial and fungal communities in Panax ginseng-growing soil. *BMC Microbiol* 2022;**22**:77.

Wright MH, Farooqui SM, White AR *et al.* Production of manganese oxide nanoparticles by Shewanella species. *Appl Environ Microbiol* 2016;**82**:5402–9.

Xu H, Song G, Yang S *et al.* Benthic nitrogen cycling in the deep ocean of the Kuroshio Extension Region. *Front Mar Sci* 2022;**9**:1–18.

Xu Y, Morel FMM. Cadmium in marine Phytoplankton. In: Sigel A, Sigel H, Sigel RKO. (eds.), *Cadmium: From Toxicity to Essentiality*. Dordrecht: Springer Netherlands, 2013,509–28.

Ye J, Coulouris G, Zaretskaya I *et al.* Primer-BLAST: a tool to design target-specific primers for polymerase chain reaction. *BMC Bioinf* 2012;**13**:134.

Yoon S, Cruz-García C, Sanford R *et al.* Denitrification versus respiratory ammonification: environmental controls of two competing dissimilatory NO3(-)/NO2(-) reduction pathways in Shewanella loihica strain PV-4. *ISME J* 2015;**9**:1093–104.

Yu X, Zhao J, Liu X *et al.* Cadmium pollution impact on the bacterial community structure of arable soil and the isolation of the Cadmium resistant bacteria. *Front Microbiol* 2021;**12**:1–11.



**Received** 31 January 2023; **revised** 19 May 2023; **accepted** 1 June 2023